Influence of Target Texture on the Deposition of Titanium Films by Long Throw Sputtering

R. Streiter [1], H. Wolf [2], P. Belsky [1], W. Tirschler [3], H. Giegengack [4] , N. Urbansky [5], T. Gessner [1,2]

[1] Chemnitz University of Technology, Center for Microtechnologies, D-09107 Chemnitz, Germany
[2] Fraunhofer Institute for Reliability and Microintegration, Dept. Micro Devices and Equipment
[3] Dresden University of Technology, Institute of Physical Metallurgy,
[4] Chemnitz University of Technology, Institute of Physics, [5] Infineon Technologies Dresden

ABSTRACT

The influence of target properties on the deposition of titanium films by long throw sputtering has been studied using Monte Carlo simulation. The precise knowledge and consideration of existing textures is shown to be a prerequisite for the correct prediction of deposition rates and the radial dependence of film thickness. The experimental investigation of target textures has been carried out both by electron back-scattering and X-ray diffraction. The emission behavior is interpreted by molecular dynamic calculations.

INTRODUCTION

Within aluminum based multilevel interconnect technology, thin titanium films deposited by PVD are used as contact layers in tungsten plug processing. Sufficient bottom coverage of the Ti is essential to achieve low contact and via resistance. On the other hand, Ti field thickness has to be kept small to avoid complications at the CMP step. As aspect ratios rise, only an increased proportion of near-normal Ti atom incidents on the wafer is therefore suitable to compensate for the decline in base coverage. The angular distribution of Ti atoms hitting the wafer is improved by increasing the distance of the target or by ionization of sputtered atoms and subsequent acceleration by an electric field. Both techniques, long throw and ionized PVD, are shown to be extendible beyond the present technology nodes [1]. Increased efforts in modeling and simulation are undertaken on different scales to optimize process conditions and to find out process limitations.

Simulation of ballistic particle transport at reactor scale is influenced by the process of atom emission from the sputter target supplying the start conditions for subsequent particle tracing. The local distribution of sputtering events depends on the strength of the parallel component of the magnetic field and can be determined from measured erosion profiles. Energy distribution may be represented by a Thompson distribution [2]. Angular distributions of sputtered atoms depend both on ion energy and target structure. In the simplest case of sputtering from amorphous or ideally isotropic polycrystalline targets at energies of a few keV the angular distribution is described by the cosine of the angle between the trajectory of the sputtered atom and the surface normal. In the sub-keV range, preferred off-normal ejection according to 'under-cosine' and heart-shaped angular distributions has been measured [3,4] and calculated [5]. Crystalline samples show preferred emission close to low index directions connecting neighboring atoms [6]. For hcp metals like Ti, such directions are <-2203> and <11-20>. This anisotropic ejection can be explained as a direct ejection in close-packed directions by head-on collisions of low-energy recoils [7,8]. The directional dependence of atom ejection from single crystal surfaces will also affect the emission behavior of polycrystalline targets having any texture, since the angular emission profile represents an average over the contributions of individual crystallites. It is generally difficult to obtain absolutely texture-free metal targets, because texture may arise from mechanical or thermal treatment during fabrication, but also as a consequence of the prolonged ion bombardment during the sputter process itself [9].

In the present paper the simulation of titanium deposition by long throw sputtering has been performed under the special consideration of the target texture. The texture was determined both by electron backscatter diffraction (EBSD) and by X-ray diffraction (XRD). The results of both investigations are compared, and the effect on the deposition rate and uniformity is discussed.

Deposition experiments using bottle-shaped test structures have been performed to check the role of target texture at feature scale as well as the validity of the assumption of unity sticking coefficient for topography simulation at the process conditions considered.

EXPERIMENTAL DETERMINATION OF TARGET PROPERTIES

Target history and process conditions

Targets TH2 and TH3 have been used in the long throw chamber of the so-called Hi-Fill module of Trikon Technologies Ltd. both for Ti and TiN deposition. Targets TU3 and TU4 have been eroded only during a process called Ultra in Trikon's extended long throw chamber [1]. The process conditions for Ti deposition are given in Table 1.

Parameter		HI-Fill	Ultra
Target distance	(cm)	24.5	44.5
Ar flow	(sccm)	20	14
Pressure	(mTorr)	1.0	0.4
Power	(kW)	7	7
Target voltage	(V)	-521	-626
Current	(A)	13	10.7

Table 1: Process conditions for Ti deposition.

Erosion profiles

The erosion profiles of the above mentioned targets have been determined by profilometric 3D surface measurement along the diameter in perpendicular directions or by digitizing the cross section. The profiles of the different targets are very similar. No significant deviations from cylindrical symmetry have been found. Fig. 1 depicts the erosion profiles after azimuthal averaging as used for simulation. The total energy applied to the targets and the volume of eroded material determined by the integration of the erosion profiles are given in Table 2. A nearly linear dependence was found.

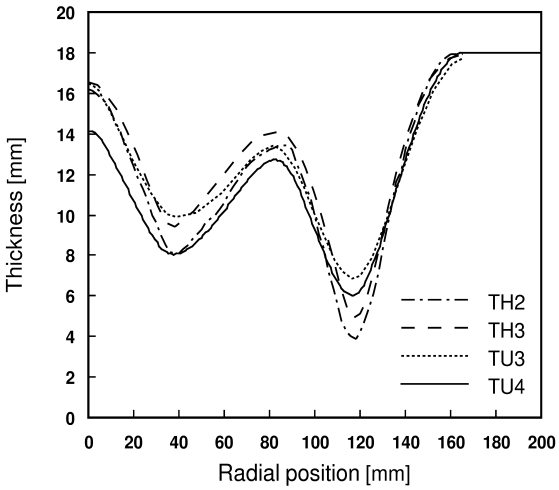

Fig. 1: Measured radial thickness distribution of the targets used.

Target		TH2	TH3	TU3	TU4
Total energy	E_t (kWh)	1900	1700	1788	1872
Target erosion	V_t (cm^3)	560	498	525	619
Sputtering yield	Y	0.43	0.42	0.51	0.53
Ion energy	$E_i/(e\ U)$	0.85	0.85	0.92	0.95

Table 2: Target erosion and calculated values of sputtering yield and reduced ion energy.

Electron backscatter diffraction

Preparation and Measurement: Five samples were cut off from target TU4 at different positions. Details of surface pretreatment and EBSD measurement have been described elsewhere [10]. The investigated samples did not show any significant differences with respect to texture and grain size.

Grain size: The average grain size was calculated by evaluating the surface area of all grains. A value of 7.75 µm was found. Applying the line section method (50 horizontal lines), an average grain size of 7.6 µm was determined with a standard deviation of 4.5 µm.

Texture: Because no significant differences between the textures of the five samples have been found, the result of the evaluation of the common data set is presented. The orientation of a total of about 20000 different grains has been determined. A pole plot representation of the target texture is depicted in Fig. 2 showing the distribution of the angles between the lattice direction <0001> of all registered grains and the axis of symmetry of the target. The pole plot shows the distribution of the mean unit deviation (mud), which is the ratio of the frequency of grains of a specific orientation to the frequency of such grains in the isotropic case (equipartition). 57 % of the grains have a <0001> direction within the angular range between 20º and 40º to the target axis.

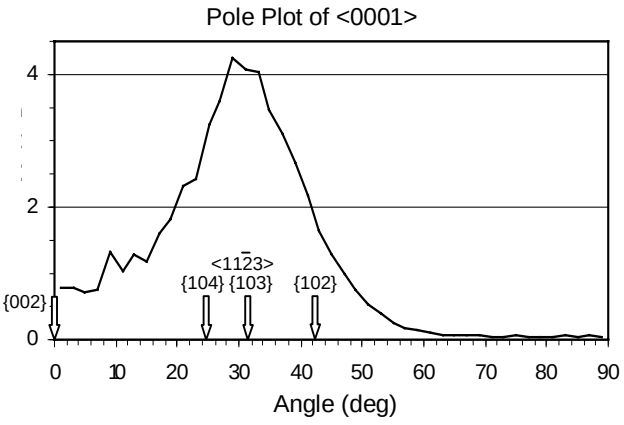

Fig. 2: EBSD pole plot representation of the target texture showing the angular distribution of the lattice direction <0001> of all registered grains.

X-ray diffraction

X-ray diffraction was applied to determine the texture of five samples cut off from target TU4. No special surface treatment was carried out. The diffraction spectra were recorded on a Seifert XRD7 diffractometer using filtered Cu K_α radiation. The samples were taken from equivalent radial positions as for EBSD investigation. The distribution of grain orientations shown in Fig. 3 has been calculated from the measured peak heights. For all samples the most pronounced reflex is associated with the lattice plane {103}. The angle between its normal and the <0001> direction is 31.4° coinciding well with the angle between the <11-23> and the <0001> direction. The corresponding component of texture is in close agreement with the results of EBSD measurement as depicted in Fig. 2. Because the angular distribution of grain orientations around the <11-23> direction has a certain width, the intensities of reflexes {102} and {104} are also enhanced. A similar distribution of texture components as measured here has been reported in Ref. [11].

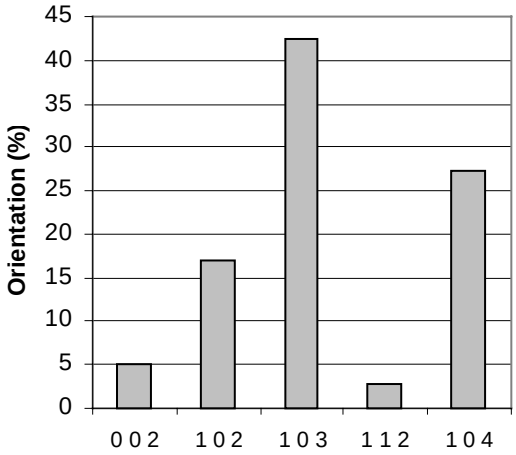

Fig. 3: Target texture measured by XRD.

SIMULATION

Basic assumptions

For the reactor scale simulation of long throw sputtering, a portable ballistic code was developed allowing the simultaneous employment of several processors for parallelized particle tracing. The code is based on the Monte Carlo approach. Because of the low pressure, the sputtered atoms undergo only a small number of scattering events between the target and the wafer. Thus, simulation can be performed applying the test particle method instead of a very time-consuming self-consistent calculation. This method implies that the state of the background gas remains unchanged from interactions with sputtered atoms allowing successive tracing. Another consequence of the low pressure is the relatively small influence of the details of the scattering model. The scattering events can be described using either the variable hard sphere (VHS) model [12] or the improved scattering angle model M1 [13]. Velocity-dependent scattering cross-sections, fitted to the Lennard-Jones and to the Abrahamson molecular interaction potential, are optionally available for argon. The combination of M1 model and Abrahamson potential best represents both viscosity data and diffusion coefficients [13] and is, therefore, preferably used for simulation.

The specification of boundary conditions includes the determination of the local distribution of sputtering events as well as of the angular and energy distribution of sputtered particles. The local distribution of sputtering events is calculated from the erosion profiles depicted in Fig. 1. For the angular and energy distribution a simplified separated description is used.

$$\phi(\vartheta, E)\, d\Omega\, dE \sim \psi(\vartheta) \cdot E\,(E + E_b)^{-3} \left(1 - \sqrt{\frac{E_b + E}{\lambda E_i}}\right) d\Omega\, dE \qquad \lambda = \frac{4\, M_t\, M_i}{(M_t + M_i)^2} \tag{1}$$

The energy part is represented by the Thompson distribution [2], where E_i is the average incident ion energy, λE_i the maximum recoil energy, and E_b the surface binding energy (approximately the heat of sublimation). λ is the fraction of the maximum transferable energy on binary collisions depending on the

target and ion species atomic masses M_t and M_i . The energy distribution reaches its maximum near $E_b/2$. Ion energy E_i does usually not directly correspond to the applied target voltage. The value of E_i can be determined from the volume of eroded target material as described below.

Because of the measured target texture the angular distribution $\psi(\vartheta)$ cannot be represented by the cosine distribution. An empirical representation $\psi_{opt}(\vartheta)$ has been used instead, which was fitted to measured rate and uniformity data. Additionally, an angular distribution $\psi_{md}(\vartheta)$ has been composed of

contributions associated with the main texture components {002},{102},{103}, and {104} identified by XRD (Fig. 3).

$$\psi_{md}(\vartheta) = a_1\,\psi_{002}(\vartheta) + a_2\,\psi_{102}(\vartheta) + a_3\,\psi_{103}(\vartheta) + a_4\,\psi_{104}(\vartheta) \qquad (2)$$

$\psi_{hkl}(\vartheta)$ are the angular distributions of atom emission from the respective crystalline surfaces calculated using the molecular dynamics code Calypso [14]. Coefficients a_i are related to the frequency of the respective surfaces and have been determined by integration of the angular distribution depicted in Fig. 2 around the inclination angle of the respective lattice planes. The resulting values of the coefficients are $a_1 = 0.11$, $a_2 = 0.16$, $a_3 = 0.38$, and $a_4 = 0.35$. Fig. 4 shows the angular distributions used for simulation and its constituents.

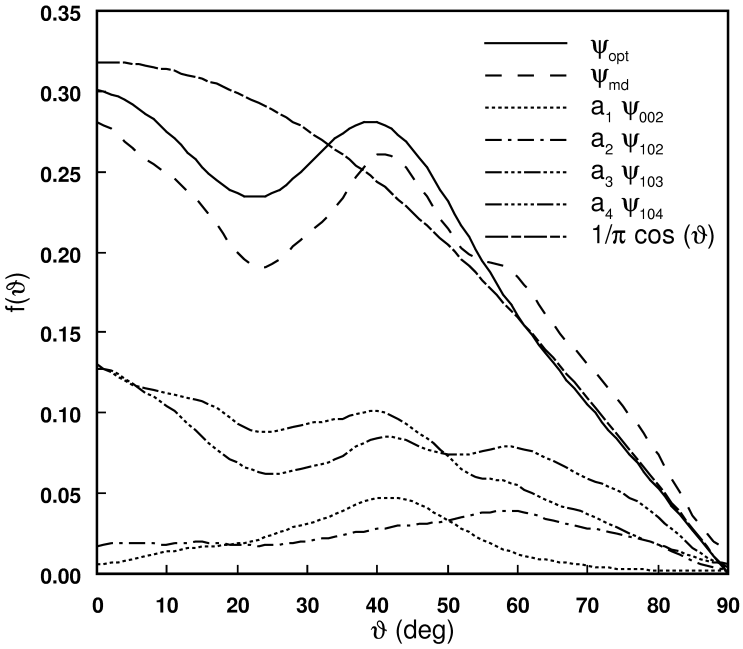

Fig. 4: Angular distributions $\psi_{opt}(\vartheta)$, $\psi_{md}(\vartheta)$, and $\psi_{hkl}(\vartheta)$.

Ion energy

If the sputtering yield is known, the actual average ion energy can be determined by iteration using the semi-empirical equation developed by Matsunami,Yamamura and Itoh [15,16] for sputtering. The sputtering yield can be calculated using the equation

$$Y = \left(\rho_t \cdot \frac{V_t}{M_t} \cdot N_A \right) \Big/ \left(\frac{E_t}{e \cdot U \cdot (1 + \gamma_{SE})} \right) \qquad (3)$$

if the target was utilized under constant process conditions. ρ_t is the mass density of the target, V_t is the volume of eroded target material, and N_A is Avogadro's number. E_t is the total energy applied to the erosion of V_t, U is the total target voltage applied, and e is the elementary charge. γ_{SE} is the secondary electron emission coefficient considering the contribution of electrons to the total current. γ_{SE} can be estimated for clean surfaces according to $\gamma_{SE} \approx 0.016\ eV^{-1}\ (\varepsilon_i - 2\,\varepsilon_F)$ [17], where ε_i and ε_F are the ionization energy of the ion and the Fermi energy of the target material, respectively. For Ar^+ and Ti, a value of about 0.1 is obtained for γ_{SE}, which is reduced in the case of surface contamination. The values of the sputtering yield and the (reduced) ion energy have been calculated from Matsunami's formula and Eq. (3) for the targets investigated. The results are given in Table 2. The ion energy corresponds to a potential drop across the cathode sheath between 85 % and 95 % of the total target voltage applied.

Parameter		HI-Fill	Ultra
Av. energy (target)	(eV)	20.2	21.9
Av. energy (wafer center)	(eV)	15.7	18.7
Mean free path of Ti atoms	(m)	0.24	0.72
Av. collisions of Ti atoms impinging at the wafer center		1.12	0.63
Deposition rate (wafer center)			
calculated	(nm/min)	100	38
measured	(nm/min)	100	39

Table 3: Simulation results for Ti deposition.

Velocity distributions

The calculated velocity distributions of Ti atoms impinging at the center of the wafer are depicted in Fig. 5 for processes Hi-Fill and Ultra. A second peak is formed at low velocities by the scattered particles. Compared to the velocity distribution of atoms just emitted from the target, the scattering peak is higher than the Thompson peak for the Hi-Fill and lower for the Ultra case, respectively. Some statistical characteristics of the reactor scale simulation are given in Table 3.

Angular distributions

The calculated angular distributions of Ti atoms impinging at the center of the wafer are depicted in Fig. 6 for processes Hi-Fill and Ultra. Because of the low average number of collisions (cf. Table 4), the position of the two racetracks of the target are perspicuously mapped as two peaks in the distribution of the angles of incidence. With increasing pressure, the peaks broaden. Increasing the target-to-wafer distance shifts the peaks towards the direction of normal incidence. The peak height increases as a consequence of the spherical normalization.

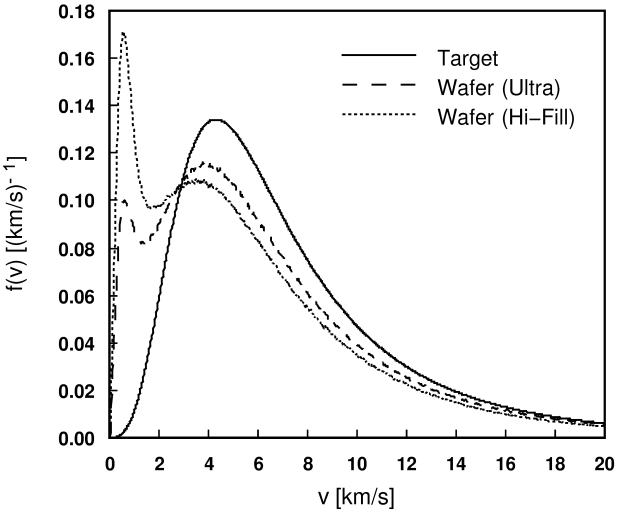

Fig. 5: Velocity distribution of Ti atoms impinging at the center of the wafer for processes Hi-Fill and Ultra in comparison with the distribution of atoms just emitted from the target.

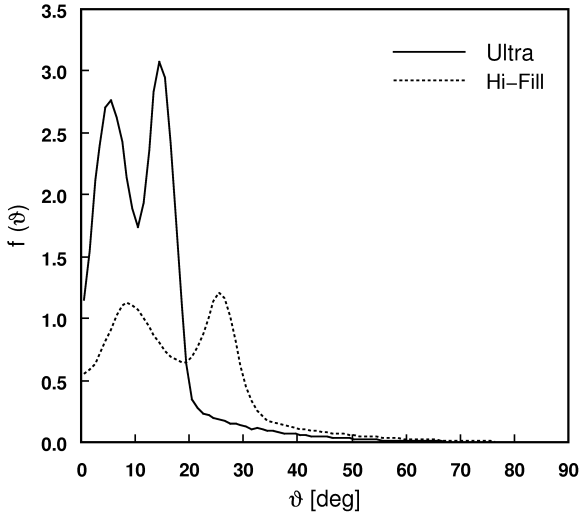

Fig. 6: Distribution of the angles of incidence ϑ' of Ti atoms at the midpoint of the wafer for processes Hi-Fill and Ultra.

Rate and Uniformity

The radial dependence of calculated film thickness normalized to the thickness at the wafer midpoint is depicted in Fig. 7 for processes Hi-Fill and Ultra in comparison with experimental results obtained from sheet resistance (Rs) measurements and from transmission electron micrographs (TEM).

If the distribution of angles of emission from the target is described by the cosine distribution, the agreement between simulation results and experimental data will be rather bad. The simulated deposition rates are generally too high. Values of 113 nm/min and 44 nm/min have been calculated at the wafer midpoint for processes Hi-Fill and Ultra, respectively. The simulation represents the measured radial course of the normalized film thickness only for the Ultra case. For the Hi-Fill process, too low a normalized film thickness is calculated at the wafer edge resulting in too bad uniformity.

Fig. 7: Radial dependence of calculated film thickness normalized to the thickness at the wafer midpoint for the Hi-Fill (lower curves) and the Ultra process (upper curves) in comparison with experimental results obtained from sheet resistance measurements (empty squares) and from transmission electron micrographs (filled squares). The distribution of the angles of emission from the target is alternatively described by the cosine distribution (dotted) and by the distribution $\psi_{opt}(\vartheta)$ (full lines) considering the target texture

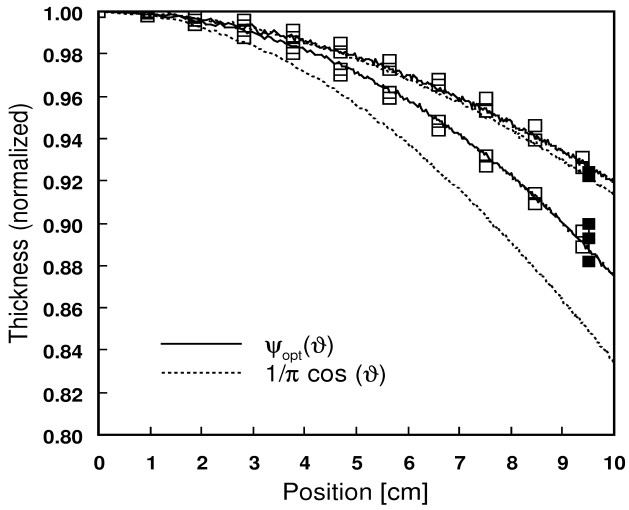

An improved representation of the experimental data will be achieved, if the influence of target texture on the emission behavior is considered. Using the angular distribution $\psi_{opt}(\vartheta)$ (Fig. 4), the simulation results are in good agreement with the measurements for both processes (cf. Table 3). Because of the enhanced sideward emission from the target, the number of atoms meeting the wafer is reduced resulting in lower deposition rates compared with the use of the cosine distribution. Moreover, the atoms preferentially ejected with polar angles around 40º contribute to an enhanced deposition at the wafer edge in the Hi-Fill case. The enhancement is negligible in the Ultra case, and the radial course of the normalized thickness is nearly the same as calculated using the cosine distribution. As shown by this example, the integration of texture effects into simulation can be a necessary prerequisite for the correct prediction of deposition rates.

Feature scale simulation

The evaluation of deposition experiments using overhang structures showed that the assumption of unity sticking coefficient is sufficient for topography simulation at feature scale for the process conditions considered. Without bias, neither reflection events nor resputtering events caused by incident Ti or fast neutral Ar have any measurable influence on film topography. Any impact of target texture on film deposition at feature scale has not been observed.

CONCLUSIONS

The simulation of long throw sputtering on reactor scale requires the precise specification of boundary conditions including the local distribution of sputtering events on the target as well as the angular and energy distribution of sputtered particles. Because of its effect on the emission behavior, the precise knowledge and consideration of existing textures is shown to be a necessary prerequisite for the correct prediction of deposition rates and the radial dependence of film thickness as well. As demonstrated for the PVD of thin titanium films, the assumption of cosine-distributed atom ejection may be sometimes inappropriate.

We acknowledge the financial support of BMBF project No. 13 N 7754.

REFERENCES

[1] D. C. Butler, K. Buchanan, S. R. Burges, N. Urbansky, S. Schmidbauer., Solid State Technology, July 2000, p. 183.
[2] M. W. Thompson, Philos. Mag. **8,** 18 (1968) 377.
[3] G. K. Wehner, D. Rosenberg, J. Appl. Phys. **31**, 1 (1960) 177.
[4] A. Malaurie, A. Bessaudou, Thin Solid Films **286** (1996) 305.
[5] H. E. Roosendaal, J. B. Sanders, Radiation Effects **52** (1980) 137.
[6] G. K. Wehner, Phys. Rev. **102** (1956) 690; J. Appl. Phys. **26** (1955) 1056.
[7] C. Lehmann, P. Sigmund, Phys. Status Solidi **16** (1966) 507.
[8] W. O. Hofer, in *Sputtering by particle bombardment III*, R. Behrisch and K. Wittmark (editors), Topics in Applied Physics Vol. 64, Springer-Verlag, Berlin, 1991, pp. 15-90.
[9] C.-F. Lo, A. Snowman, P. Gilman, R. Mathew, D. Draper, C. Fisher, VMIC 2000, http://www.materialsresearch.com/mrc/docs/tech_papers/vmic2000.ppt
[10] H. Wolf, R. Streiter, W. Tirschler, H. Giegengack, N. Urbansky, T. Gessner, Microelectron. Eng. 63 (2002) 329.
[11] C.-F. Lo, S. Kulkarni, R. Mathew, P. S. Gilman, H. Tamura, VMIC 1999, http://www.materialsresearch.com/mrc/docs/VMIC99-Ti-TiN-Al.html
[12] G. A. Bird, *Molecular gas dynamics and the direct simulation of gas flows*, Claredon , Oxford, 1994.
[13] A. Kersch, W.J. Morokoff, *Transport simulation in microelectronics*, Birkhäuser, Basel, 1995.
[14] M. A. Karolewski, Surface and Interface Analysis **29** (1999) 114.
[15] N. Matsunami et al., Atomic Data and Nuclear Data Tables **31** (1984) 1-84.
[16] Y. Yamamura, N.Itoh, in *Ion beam assisted film growth*, T. Itoh (editor), Elsevier, Amsterdam, 1989.
[17] Y. P. Raizer, *Gas Discharge Physics*, Springer, New York, 1991.